Biochemistry and Biophysics Reports 22 (2020) 100741

Contents lists available at ScienceDirect

Biochemistry and Biophysics Reports

journal homepage: www.elsevier.com/locate/bbrep

Importance of methodology in the evaluation of renal mononuclear phagocytes and analysis of a model of experimental nephritis with Shp1 conditional knockout mice

Mitsuharu Watanabe[a], Yoriaki Kaneko[a,*], Yuko Ohishi[a], Masato Kinoshita[a], Toru Sakairi[a], Hidekazu Ikeuchi[a], Akito Maeshima[a], Yasuyuki Saito[b], Hiroshi Ohnishi[c], Yoshihisa Nojima[a], Takashi Matozaki[b], Keiju Hiromura[a]

[a] Department of Nephrology and Rheumatology, Gunma University Graduate School of Medicine, 3-39-22 Showa-machi, Maebashi, Gunma 371-8511, Japan
[b] Division of Molecular and Cellular Signaling, Department of Biochemistry and Molecular Biology, Kobe University Graduate School of Medicine, 7-5-1 Kusunoki-cho, Chuo-ku, Kobe 650-0017, Japan
[c] Department of Laboratory Sciences, Gunma University Graduate School of Health Sciences, 3-39-22 Showa-machi, Maebashi, Gunma 371-8514, Japan

ARTICLE INFO

Keywords:
Macrophage
Dendritic cell
Phagocyte
Shp1
Nephritis

ABSTRACT

Tissue resident mononuclear phagocytes (Mophs), comprising monocytes, macrophages, and dendritic cells (DCs), play important roles under physiological and pathological conditions. The presence of these cells in the kidney has been known for decades, and studies of renal Mophs (rMophs) are currently underway. Since no unified procedure has been identified to isolate rMophs, results of flow cytometric analysis of rMophs have been inconsistent among studies. We therefore first evaluated a preparative method for rMophs using collagenous digestion. The yield of rMophs greatly increased after the collagenase digestion. In particular, F4/80^{high} rMophs, which were positive for CD11c, a specific marker of DCs, dramatically increased. In addition, since neutrophils are sometimes mixed among rMophs in the analysis of flow cytometry, we established a gating strategy for eliminating neutrophils. To determine the contribution of rMophs to the development of autoimmune nephritis, we analyzed an experimental model of autoimmune nephritis that was applied to Shp1 conditional knockout mice (Shp1 CKO). This knockout strain is generated by crossing a mouse line carrying floxed Shp1 allele to mice expressing Cre recombinase under the control of the CD11c promoter. Shp1 CKO therefore specifically lack Shp1 in cells expressing CD11c. As a result, Shp1 CKO were susceptible to that experimental glomerulonephritis and F4/80^{high} rMophs of Shp1 CKO increased dramatically. In conclusion, our preparative methods for collagenase digestion and gating strategy for neutrophils are necessary for the analysis of rMophs, and Shp1 suppresses the development of autoimmune nephritis through the control of rMophs.

1. Introduction

Macrophages were discovered at the end of the nineteenth century based on their phagocytic capacity. For decades, tissue-resident macrophages were believed to be continuously maintained by blood-circulating monocytes, which arose from progenitors in the bone marrow. However, this concept has been challenged recently and may represent an oversimplification. Emerging evidence suggests that two distinct populations of macrophages exist in almost all tissues: monocyte-derived macrophages, replenished by bone marrow; and tissue-resident macrophages of embryonic origin that self-renew in situ [1]. In addition, bone marrow-derived macrophages seem to represent a smaller fraction in the kidney during steady state, but might increase in number during inflammation [2].

Dendritic cells (DCs), which are the most potent antigen-presenting cells, represent another type of phagocytic cells. Macrophages, monocytes and DCs thus comprise mononuclear phagocytes (Mophs) in many organs. During the last two decades, a large number of scientists have worked on the analysis of renal diseases, focusing on the contribution of renal Mophs (rMophs), and marked progress has been achieved

Abbreviations: Mophs, mononuclear phagocytes; rMophs, renal Mophs; Shp1 CKO, Shp1 conditional knockout mice; I/R, ischemia-reperfusion; BSA, bovine serum albumin; M-CSF, macrophage colony-stimulating factor

* Corresponding author.
E-mail address: ykaneko-gunma@umin.ac.jp (Y. Kaneko).

https://doi.org/10.1016/j.bbrep.2020.100741
Received 10 November 2019; Received in revised form 24 January 2020; Accepted 27 January 2020

together with the development of flow cytometry [3].

However, since the preparative method for isolating rMophs is not well established, the yields of rMophs have differed between experiments [4–6]. We found that the major reason for the variability of results arises from whether enzymatic digestion is applied. Historically, DCs were found by Ralph Steinman in 1973; during the discovery of DCs, he noticed that collagenase treatment of lymphoid tissue allowed a more consistent yield of DCs than mechanical dissection [7]. A combination of density centrifugation and collagenase treatment is thus the standard procedure to collect DCs from lymphoid tissues [8]. Nowadays, enzymatic digestion using collagenase is becoming popular to collect single cells from the kidney [4,6,9,10]. However, mechanical dissociation of the kidney was a common method of isolating Mophs from the kidney 10 years ago [11,12], and is still employed for flow cytometric analysis of rMophs [5,13].

To characterize the contribution of rMophs to kidney diseases, the ability to identify subpopulations of rMophs correctly is crucial. For this reason, rMophs are classified depending on the following cell surface antigens: F4/80, MHCII, CD11b, CD11c, Ly6C, Ly6G, and CX3CR1. In general, $CD45^+$ hematopoietic cells residing in the kidney and showing positivity for CD11b, CD11c, or F4/80 are considered as rMophs. Furthermore, the combination of these three molecules is useful to delineate subpopulations of rMophs. In 2013, Kawakami et al. reported rMophs are able to be divided into five distinct subpopulations according to the expression patterns of CD11b, F4/80 and CD11c [6].

Although flow cytometry is a powerful tool to identify subpopulations of rMophs, the results of studies often appear varied and inconsistent, because no definitive gating strategy for the identification of rMophs has been established. In particular, rMophs are identified as cells that express CD11b and Ly6C; however, these two molecules are known to be expressed on neutrophils. Neutrophils thus could be mixed among rMophs unless Ly6G, a neutrophil-specific marker, is used for the elimination of neutrophils. For instance, in the analysis of ischemia-reperfusion (I/R), a widely used model of acute kidney injury, neutrophils are known to increase in the early stages of this model. However, rMophs are analyzed without eliminating neutrophils [10,14]. In the murine model of unilateral ureteral obstruction, a commonly used murine model for the analysis of renal fibrosis, rMophs that could include neutrophils are analyzed as in the I/R models [15,16]. Collectively, evaluation by flow cytometry is needed to confirm whether neutrophils are mixed among rMophs. The gating strategy for eliminating neutrophils is important to analyze the function of rMophs.

The nonreceptor-type protein tyrosine phosphatase Shp1 contains two tandem Src homology 2 domains, and is highly expressed in hematopoietic cells including DCs. Shp1 plays an inhibitory role in signaling pathways. Indeed, the mouse mutant motheaten (*me/me*), which harbors mutations in the Shp1 gene (*Ptpn 6*), shows chronic inflammation and dies at an early age from interstitial pneumonitis [17]. Although many studies have addressed immunological disorders in motheaten mice, less is known about the functional abnormality of DCs. For this reason, we generated Shp1 conditional knockout mice (Shp1 CKO), in which Shp1 was specifically ablated in $CD11c^+$ cells, and found that splenic $CD4^+$ T cells from Shp1 CKO are prone to differentiate into Th1 cells. At 36–40 weeks old, Shp1 CKO develop glomerulonephritis characterized by the deposition of immunoglobulin (Ig)G and complement component 3 [18].

In the present study, we examined the importance of methodology in the evaluation of rMophs and investigated the contribution of rMophs to the development of autoimmune nephritis. We first compared collagenase treatment to mechanical digestion in terms of the efficiency of collecting rMophs. We then characterized neutrophils mixed among rMophs by flow cytometry. We next induced the model of experimental autoimmune nephritis in young Shp1 CKO that do not manifest clinically evident glomerulonephritis and assessed the susceptibility of young Shp1 CKO to the experimental nephritis. Finally, we analyzed phenotypic changes in rMophs for Shp1 CKO.

2. Materials & methods

2.1. Mice

C57BL/6j mice were purchased from Charles River Japan (Kanagawa, Japan), and female mice at 8–10 weeks old were used. To generate $Ptpn6^{fl/fl}$; CD11c-*Cre* mice (Shp1 CKO), $Ptpn6^{fl/fl}$ mice were crossed to CD11c-*Cre* mice purchased from The Jackson Laboratory (Bar Harbor, ME) as described elsewhere [18,19]. Sex- and age-matched $Ptpn6^{fl/fl}$ littermates without *Cre* gene were studied as controls. Floxed *Ptpn6* and *Cre* alleles were detected by PCR as described previously [18]. All mice were bred and maintained in the Institute of Experimental Animal Research at Gunma University, Japan, under specific pathogen-free conditions. Mice were handled in accordance with protocols approved by the Animal Care Committee of Gunma University. All animal experiments complied with ARRIVE guidelines.

2.2. Antibodies and reagents for flow cytometry

FITC-conjugated monoclonal antibodies (mAbs) to mouse Ly6G (1A8); PE-conjugated mAbs to mouse F4/80 (BM8), CD11b (M1/70) and Ly6C (HK1.4); PE-Cy7-conjugated mAbs to mouse F4/80 (BM8) and CD11b (M1/70); APC-conjugated mAbs to mouse CD45.2 (104), CD11b (M1/70) and Ly6C (HK1.4); APC-Cy7-conjugated mAbs to mouse CD11c (N418) and CD45.2 (104) were obtained from Biolegend (San Diego, CA). Propidium iodide (PI) solution was obtained from Sigma-Aldrich (St. Louis, MO).

2.3. Histopathology

For all histological analyses, bilateral kidneys were removed from the mice perfused with cold PBS. The kidneys were fixed in 4% paraformaldehyde PBS, then embedded in paraffin. Four-micrometer sliced sections from the kidneys were stained with periodic acid-Schiff. For histochemical detection of F4/80, kidneys embedded in OCT compound were frozen in liquid nitrogen and stored at −70 °C. Five-micrometer cryostat sections of the kidney were fixed with cold methanol/acetone and treated for 10 min in 0.3% hydrogen peroxide in PBS to block endogenous peroxidase-like activity. After reducing endogenous biotin activity using an avidin/biotin blocking kit (Nichirei Bioscience Inc., Tokyo, Japan), sections were incubated with biotinylated primary antibodies followed by streptavidin-conjugated HRP. TSA Biotin Systems (PerkinElmer, Waltham, MA) was used to increase staining sensitivity according to the instructions from the manufacturer. Color development was performed using diaminobenzidine tetrahydrochloride solution (Nichirei Bioscience Inc.). All images were acquired under light microscopy (BZ-X700; Keyence, Osaka, Japan).

2.4. Preparation of rMophs

The protocol for the preparation of splenic DCs described elsewhere was modified slightly using a gentleMACS Dissociator (Miltenyi Biotec, Bergisch Gladbach, Germany) [20]. In brief, bilateral kidneys were removed from the mice perfused with cold PBS. The kidneys were then injected with Hank's balanced salt solution containing 400 U/ml collagenase (Wako Pure Chemical Industries, Osaka, Japan) and 50 μg/ml DNase I (Roche, Basel, Switzerland). The kidneys were then placed in gentleMACS C Tubes (Miltenyi Biotec) with the digestion solution for 50 min at 37 °C and minced using the gentleMACS Dissociator. The digested cell suspension was passed through a 40-μm polyester mesh and the sieved cells were suspended in PBS containing 40% percoll (GE Healthcare, Chicago, IL) and overlaid onto 70% percoll. The resulting gradient was centrifuged at 750 × *g* for 20 min at 20 °C, after which the cells at the interface of the two layers were collected. To evade

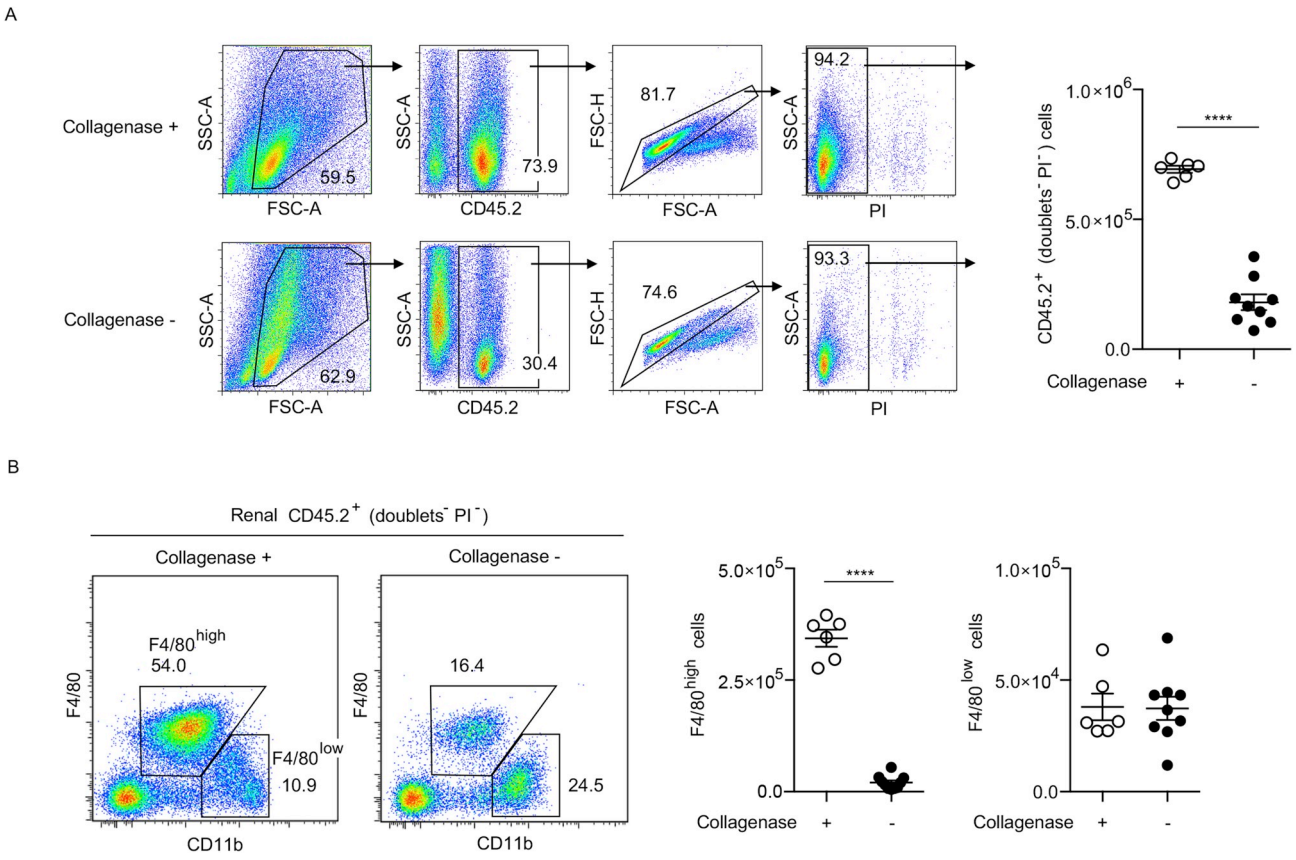

Fig. 1. The yield of F4/80^{high} cells strongly depends on collagenase treatment.
(**A**) Comparison of the yields of CD45.2^{+} hematopoietic cells from kidney prepared with or without collagenous treatment. Mononuclear cells prepared after collagenase treatment (Collagenase +) and mechanical dissociation (Collagenase -) are shown in the upper and lower panels, respectively. The right graph shows the absolute numbers of CD45.2^{+} mononuclear cells prepared by different methods. (**B**) Representative dot plots of CD11b vs. F4/80 expression in CD45.2^{+} cells isolated as above. Two major populations are identified in the plots: F4/80^{high}/CD11b^{dull} (F4/80^{high}) cells; and F4/80^{low}/CD11b^{high} (F4/80^{low}) cells. The absolute number of each fraction is shown in the right graphs. Data represent mean ± SEM. Circles represent the number of cells in a mouse. A total of six mice in the collagenase+ group and nine in the collagenase– group were examined. Three independent experiments were combined. ****P < 0.0001, by unpaired, two-tailed Student's *t*-test.

collagenase treatment, the kidneys from PBS-perfused mice were directly minced with the gentleMACS Dissociator, and these mechanically dissociated cells were subjected to percoll gradient separation.

2.5. Flow cytometry and cell sorting

To minimize nonspecific bindings of mAbs, single-cell suspensions were preincubated with anti-mouse CD16/CD32 mAb (BD Pharmingen, San Jose, CA), then washed and incubated with the indicated mAb conjugates for 15 min on ice. The stained cells were resuspended in staining buffer containing 1 μg/ml PI for the elimination of dead cells. Flow cytometry was performed using an Attune Acoustic Focusing Cytometer (Applied Biosystems, Foster City, CA), and all data were analyzed using FlowJo software (FlowJo LLC, Ashland, OR). The absolute number of cells infiltrating into the kidney was quantified by flow cytometry using CountBright absolute counting beads (Life Technologies, Waltham, MA) following the instructions from the manufacturer. For cell sorting of renal Ly6G^{+} cells, single-cell suspensions were stained with FITC-Ly6G, PE-CD11b, PI and PE-Cy7-F4/80. Ly6G^{+} cells among the CD11b^{+}/F4/80^{low} population were then sorted using an S3 Cell Sorter (Bio-Rad, Hercules, CA). Sorted cells were stained with May-Grünwald -Giemsa, and cell morphology was captured under light microscopy (BX51 microscope; Olympus, Tokyo, Japan).

2.6. Induction of experimental glomerulonephritis

The protocol for the induction of experimental glomerulonephritis by repeated administration of bovine serum albumin (BSA) has been described elsewhere [21]. Briefly, 8- to 10-week-old female controls or Shp1 CKO were immunized by subcutaneous injection with 0.2 mg of BSA (Sigma-Aldrich) in complete Freund's adjuvant (CFA) (Wako Pure Chemical Industries, Osaka, Japan) at 2-week intervals. Flow cytometric and histological studies of the kidney were performed at 8 weeks after the first injection of BSA. Serum creatinine and serum albumin levels were evaluated at the same time. Proteinuria was monitored every other week. As a control, CFA without BSA was injected at the same intervals.

2.7. Serum and urine analysis

For measurement of the levels of serum creatinine and serum albumin, serum samples were assessed using a Hitachi 7180 autoanalyzer (Hitachi High-Technologies Corporation, Tokyo, Japan). Urine albumin levels were measured using Albustix (Siemens Healthcare Diagnostics, Erlangen, Germany) according to the following scores: -, negative; ±, 15 mg/dl; 1+, 30 mg/dl; 2+, 100 mg/dl; 3+, 300 mg/dl; and 4+, 1000 mg/dl.

2.8. Statistical analysis

Data are presented as means ± standard error of the mean (SEM). Differences between the two groups were analyzed using a two-tailed Student's *t*-test. Differences among multiple groups were analyzed by one-way analysis of variance (ANOVA). If ANOVA revealed

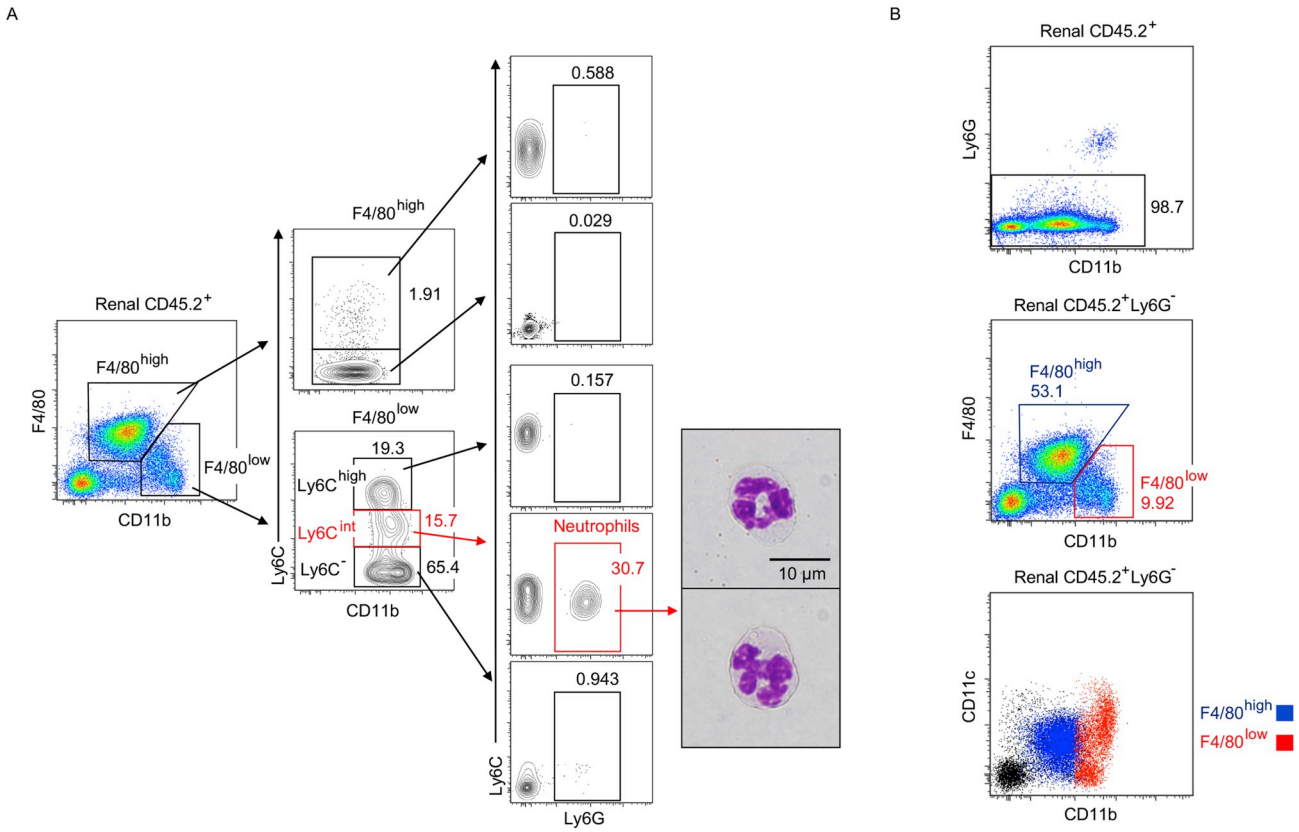

Fig. 2. Establishment of a gating strategy for the identification of rMophs.
(**A**) Neutrophils in F4/80^{low} cells are identified as Ly6C^{int}/Ly6G^{+} cells. Representative images of the sorted cells stained with May-Grünwald -Giemsa solution are shown in the right photos. (**B**) Gating strategy for the identification of rMophs. CD45.2^{+} cells from the kidney with collagenase treatment were analyzed. Ly6G^{+} cells were excluded. Blue and red dots in the bottom panel represent F4/80^{high} and F4/80^{low} rMophs in the middle panel, respectively. The following mixture of antibodies was used: CD45.2, CD11b, F4/80, Ly6G and CD11c. A total of six mice were examined in three independent experiments. (For interpretation of the references to colour in this figure legend, the reader is referred to the Web version of this article.)

significance, Bonferroni's post-hoc test was applied. Statistical analysis was performed using GraphPad Prism 6 software (GraphPad Software, La Jolla, CA). Values of $P < 0.05$ were considered statistically significant.

3. Results

3.1. Collagenase treatment increases the yield of F4/80^{high} rMophs

We first evaluated the preparative method of mononuclear cells from the kidney with enzymatic digestion, compared that with mechanical dissociation. The population containing rMophs was first determined in an FSC vs. SSC dot plot by reference to that of splenocytes to eliminate the majority of parenchymal cells of the kidney from mononuclear cells (Fig. 1A). After that, CD45.2^{+} (hematopoietic) cells were gated, then doublets and dead cells were excluded. Consequently, collagenase digestion appeared superior for collecting CD45.2^{+} cells from the kidney, compared to mechanical dissociation (Fig. 1A).

Once CD45.2^{+} cells were successfully isolated from the kidney, we next identified the two major subsets of rMophs with the use of antibodies against CD45.2, CD11b and F4/80. The F4/80^{high} and F4/80^{low} rMoph subpopulations were determined in the dot plot of CD11b vs. F4/80 that was gated in CD45.2^{+} cells. Regarding the influence of the collagenase treatment on the acquisition of cells from different subpopulations, the yield of F4/80^{low} rMophs did not differ between methods. However, the absolute number as well as the percentage of F4/80^{high} rMophs obtained after collagenase digestion was much greater than that after mechanical dissociation (Fig. 1B). These results indicate that collagenase digestion is favorable when collecting rMophs.

3.2. Establishment of the gating strategy to identify rMophs

We next analyzed the details of the two fractions of rMophs, F4/80^{high} and F4/80^{low} rMophs, after establishment of the isolating method using collagenase. Since neutrophils are mixed among rMophs [10], eliminating neutrophils from among rMophs is important to avoid misinterpretation of the results. We therefore tried to identify neutrophils, which are positive for Ly6C^{int}/Ly6G^{+}, among F4/80^{high} and F4/80^{low} rMophs. F4/80^{low} rMophs were able to be divided into three subpopulations based on expression levels of CD11b and Ly6C (Fig. 2A); among these, the Ly6C^{int}/Ly6G^{+} subpopulation, corresponding to the fraction containing neutrophils, was clearly segregated. To confirm the morphological appearance of Ly6C^{int}/Ly6G^{+} cells, the cells in this fraction were sorted and stained with May-Grünwald -Giemsa. As a result, microscopic analysis of the selected cells revealed the characteristic features of neutrophils (Fig. 2A). These findings confirm that a significant number of neutrophils are mixed among F4/80^{low} cells.

To determine expression levels of CD11c, we analyzed this molecule in the subpopulations of F4/80^{high} and F4/80^{low} rMophs after gating out Ly6G^{+} cells. The former cells expressed intermediate levels of CD11c on the cell surface; conversely, the latter contained two subpopulations, CD11c^{high} and CD11c^{-} (Fig. 2B). Collectively, CD45.2^{+} renal mononuclear cells that express either CD11b, CD11c, or F4/80, but not Ly6G, are hereafter referred to as rMophs.

3.3. F4/80^{high} rMophs are increased in the experimental nephritis induced in Shp1 CKO

Since we found that F4/80^{high} rMophs express CD11c, we examined Shp1 expression in F4/80^{high} rMophs. We isolated F4/80^{high} rMophs from Shp1 CKO by magnetic beads and analyzed the recombination of Shp1 alleles by PCR. As a result, the purity of MACS-sorted F4/80^{high} rMophs from either control or Shp1 CKO consistently exceeded 95%. Shp1 alleles were actually depleted in F4/80^{high} rMophs from Shp1 CKO (Supplementary Fig. 1). These findings were consistent with results for splenic DCs expressing CD11c on the cell surface [18].

We confirmed that F4/80^{high} rMophs from Shp1 CKO lack Shp1, then applied a model of experimental autoimmune nephritis to young Shp1 CKO. This model corresponds to glomerulonephritis with vasculitis in humans, and was induced by repeated immunization of BSA in CFA for 8 weeks at 2-week intervals, followed by daily intraperitoneal

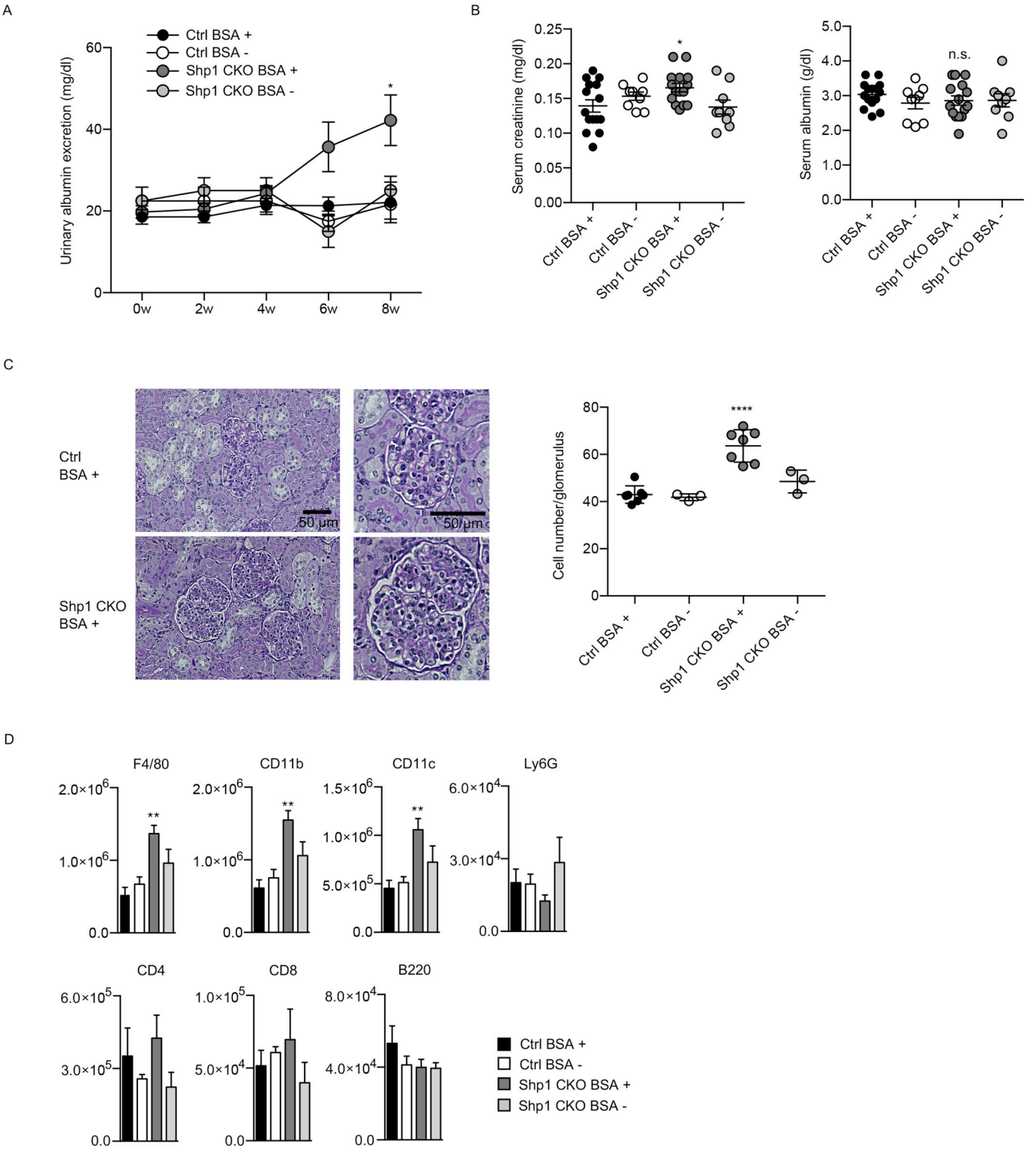

(caption on next page)

Fig. 3. Shp1 CKO are more susceptible to experimental glomerulonephritis.
(**A**) Levels of urinary albumin excretion of controls and Shp1 CKO after BSA immunization. Albuminuria was determined every two weeks after the first injection of BSA. Data represent mean ± SEM. Controls and Shp1 CKO injected with BSA in CFA are denoted as Ctrl BSA + and Shp1 CKO BSA +, respectively. The mice injected with only CFA are denoted as Ctrl BSA - or Shp1 CKO BSA -. The numbers of mice used at each time point in Ctrl BSA +, Ctrl BSA -, Shp1 CKO BSA +, and Shp1 CKO BSA - are 19–26, 6–9, 21–27, and 6–9, respectively. (**B**) Serum creatinine and albumin levels in the mice at 8 weeks after the first immunization. Data represent mean ± SEM. The numbers of mice used in Ctrl BSA +, Ctrl BSA -, Shp1 CKO BSA +, and Shp1 CKO BSA - are 15, 9, 15, and 9, respectively. (**C**) Light microscopic images of renal sections from Ctrl BSA + or Shp1 CKO BSA + at 8 weeks after the first immunization stained by periodic acid-Schiff. Images are representative of the sections from seven mice in each group. For quantitative assessment of glomerular pathology, glomerular cellularity was examined by counting the number of cells with nuclei per glomerulus, as described previously (right graph) [18]. Twenty glomeruli of similar size were examined for each animal. Data represent mean ± SEM. The numbers of mice used in Ctrl BSA +, Ctrl BSA -, Shp1 CKO BSA +, and Shp1 CKO BSA - are 7, 3, 7, and 3, respectively. (**D**) Quantification of the number of inflammatory cells infiltrating into the kidney. Mononuclear cells prepared with collagenase digestion were quantified by flow cytometry using counting beads. The absolute numbers of CD45.2^{+} cells positive for F4/80, CD11b, CD11c, Ly6G, CD4, CD8 and B220 in a mouse were determined. The mice at 8 weeks after the first immunization were analyzed. Data represent mean ± SEM. The numbers of mice used in Ctrl BSA +, Ctrl BSA -, Shp1 CKO BSA +, and Shp1 CKO BSA - are 4, 3, 4, and 3, respectively. *P < 0.05, **P < 0.01, ****P < 0.0001 vs. Ctrl BSA +. One-way ANOVA was followed by Bonferroni's test.

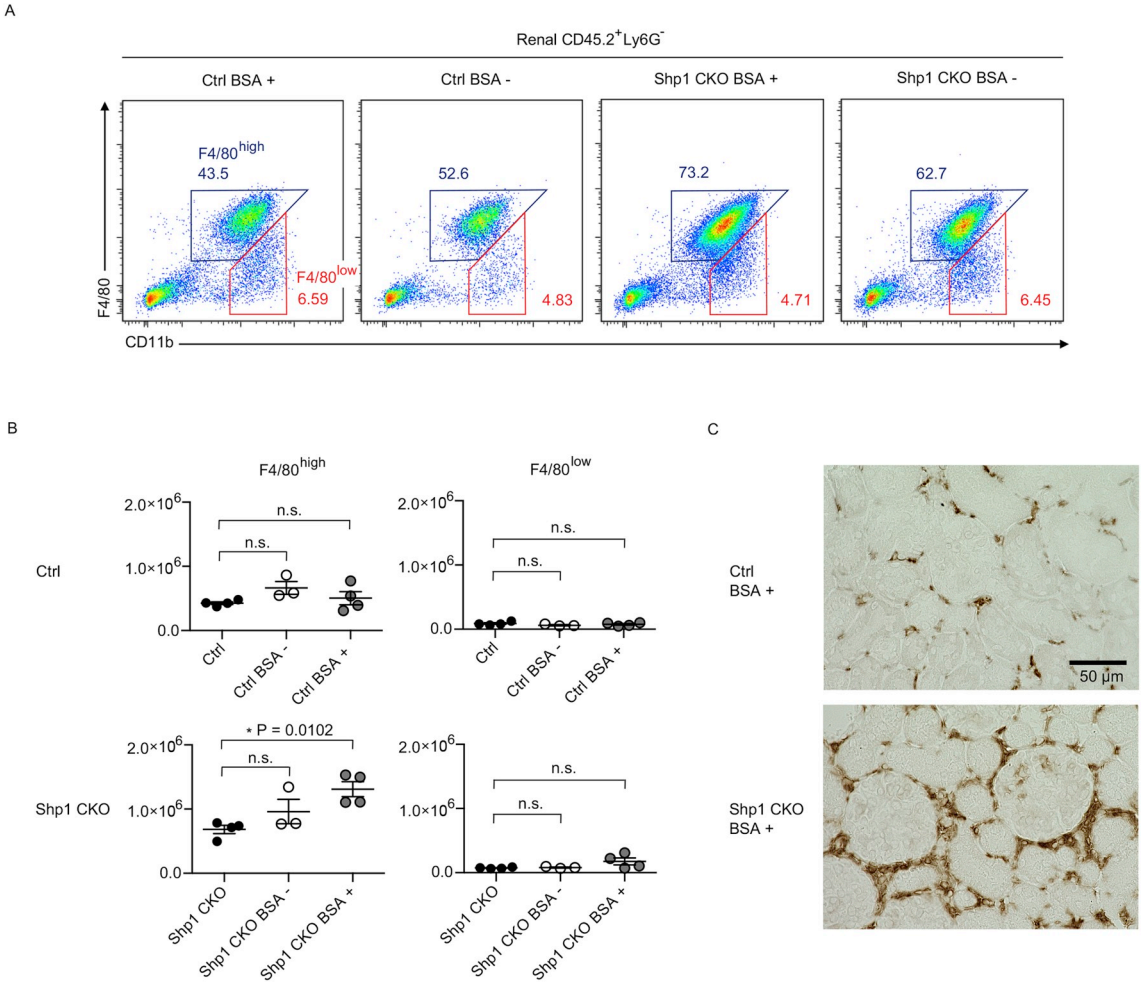

Fig. 4. F4/80^{high} rMophs increase in Shp1 CKO with glomerulonephritis.
(**A**) Representative dot plots of CD11b vs. F4/80 expression in CD45.2^{+}/Ly6G^{-} cells from the kidney of controls or Shp1 CKO at 8 weeks after the first immunization. Blue squares indicate F4/80^{high} rMophs and red squares indicate F4/80^{low} rMophs. (**B**) Quantification of the number of F4/80^{high} and F4/80^{low} rMophs in a mouse from each group at 8 weeks after the first immunization. Controls and Shp1 CKO immunized with BSA in CFA or CFA alone were analyzed. In addition, age-matched controls and Shp1 CKO without treatment, denoted as Ctrl and Shp1 CKO, respectively, were analyzed as normal controls. Data represent mean ± SEM. The numbers of mice immunized with BSA in CFA and with CFA alone are four and three, respectively. The numbers of mice in controls and Shp1 CKO without treatment are four each. One-way ANOVA was followed by Bonferroni's test. (**C**) Immunohistochemical staining for F4/80 of renal sections from controls or Shp1 CKO at 8 weeks after the first BSA immunization. Images are representative of findings from four mice per group. (For interpretation of the references to colour in this figure legend, the reader is referred to the Web version of this article.)

injection of BSA. In normal mice, no proteinuria is observed until the beginning of daily injection, whereas Shp1 CKO developed mild but significant albuminuria 8 weeks after the first immunization (Fig. 3A). Moreover, Shp1 CKO developed renal impairment with an increase in serum creatinine at that time (Fig. 3B). In histopathological analyses, marked proliferative glomerulonephritis was observed in BSA-immunized Shp1 CKO, which led to the significant increase in glomerular cellularity (Fig. 3C). These results demonstrate that Shp1 CKO are highly susceptible to experimental glomerulonephritis. Quantification of the number of inflammatory cells in the kidneys of immunized mice

at the end of repeated immunization showed that cells positive for F4/80, CD11b, and CD11c were increased in the kidney of Shp1 CKO (Fig. 3D).

We found inflammatory cells positive for rMoph-related markers in the kidney of Shp1 CKO, and next determined phenotypic changes in rMophs for Shp1 CKO. Representative dot plots of rMophs from the mice that received repeated injection of CFA with or without BSA are shown in Fig. 4A. Proportions and absolute numbers of F4/80^{high} rMophs in BSA-immunized Shp1 CKO were both increased 8 weeks after the start of immunization, but the number of F4/80^{low} rMophs of Shp1 CKO barely changed (Fig. 4A and B). To confirm the location of cells expressing F4/80 in the kidneys of BSA-immunized Shp1 CKO, we performed immunohistochemical analysis. As a result, the majority of F4/80-expressing cells were found in the periglomerular area, whereas a smaller number was observed in the glomeruli of BSA-immunized Shp1 CKO (Fig. 4C).

4. Discussion

We have shown that the preparative method for rMophs clearly influences the yield of these cells. In particular, collagenase digestion is useful to collect F4/80^{high} rMophs. Although F4/80 and CD11b are specific markers for macrophages, and CD11c is a specific marker for DCs, the majority of rMophs expressed F4/80, CD11b and CD11c on the cell surface at the same time (Fig. 2B). This result suggests that the majority of rMophs are not clearly classifiable into macrophages or DCs. Indeed, rMophs are reported to have antigen-presenting capability, correlating well with the expression levels of CD11c [6]. The majority of rMophs therefore possess overlapping characteristics of macrophages and DCs. Collectively, collagenase treatment favorable to isolate DCs should be used to collect rMophs.

Concerning the importance of the gating strategy in identifying rMophs, we found that neutrophils accounted for over 30% of the CD11b^{high}/Ly6C^{int} subpopulation among F4/80^{low} rMophs from normal kidneys. Given the increased numbers of neutrophils circulating in the blood in inflamed tissue, we should carefully assess the results of flow cytometric analyses for diseased kidneys. Collectively, careful exclusion of neutrophils from among rMophs using the neutrophil-specific marker Ly6G is required for appropriate evaluation.

To analyze rMophs that influence the development of autoimmune glomerulonephritis, we applied an experimental nephritis model in Shp1 CKO. We then found that Shp1 CKO were susceptible to immunization with BSA and showed mild but significant proteinuria. In addition, F4/80^{high} rMophs increased in Shp1 CKO after the onset of nephritis. Since F4/80^{high} rMophs expressed significant levels of CD11c, which leads to the specific depletion of Shp1 in F4/80^{high} rMophs of Shp1 CKO, F4/80^{high} rMophs could be more activated than those of control mice. The loss of Shp1 and consequent activation of rMophs would thus explain the disease susceptibility of Shp1 CKO and an increase in F4/80^{high} rMophs in Shp1 CKO.

Macrophage colony-stimulating factor (M-CSF) is a growth factor that controls the function of tissue-resident macrophages, and with the analysis of bone marrow-derived macrophages from *me/me* mice, Chen et al. found the hyperproliferation of macrophages and hyperphosphorylation of M-CSF receptors in response to M-CSF [22]. These results indicate that Shp1 acts as a negative regulator of M-CSF signaling. The increase of rMophs in Shp1 CKO can therefore be accounted for by the hyperactivation of the signaling pathway in rMophs to M-CSF.

In the present study, we have shown that collagenase treatment is necessary to isolate F4/80^{high} rMophs and our gating strategy is useful to analyze rMophs. We also found that the depletion of Shp1 in CD11c^{+} cells enhanced the susceptibility of autoimmune nephritis with an increase in F4/80^{high} rMophs. We believe that our findings will prove important in elucidating the mechanisms underlying kidney diseases.

Funding

This work was supported by JSPS KAKENHI Grant Numbers JP16K09887 (Y.K.), JP19K08902 (Y.K.), and JP18K08231 (K.H.).

CRediT authorship contribution statement

Mitsuharu Watanabe: Investigation, Writing - original draft. **Yoriaki Kaneko:** Conceptualization, Writing - original draft, Supervision. **Yuko Ohishi:** Investigation. **Masato Kinoshita:** Investigation. **Toru Sakairi:** Validation. **Hidekazu Ikeuchi:** Validation. **Akito Maeshima:** Validation. **Yasuyuki Saito:** Validation. **Hiroshi Ohnishi:** Validation, Writing - original draft. **Yoshihisa Nojima:** Validation. **Takashi Matozaki:** Writing - original draft, Supervision. **Keiju Hiromura:** Supervision.

Declaration of competing interest

The authors declare no conflict of interest.

Acknowledgements

We thank B.G. Neel and L.I. Pao for providing us *Ptpn6*$^{fl/fl}$ mice; R. Koitabashi and A. Saito for their technical assistance.

Appendix A. Supplementary data

Supplementary data to this article can be found online at https://doi.org/10.1016/j.bbrep.2020.100741.

References

[1] F. Ginhoux, M. Guilliams, Tissue-resident macrophage ontogeny and homeostasis, Immunity 44 (2016) 439–449, https://doi.org/10.1016/j.immuni.2016.02.024.
[2] S.F. Viehmann, A.M.C. Böhner, C. Kurts, S. Brähler, The multifaceted role of the renal mononuclear phagocyte system, Cell. Immunol. 330 (2018) 97–104, https://doi.org/10.1016/j.cellimm.2018.04.009.
[3] P.M. Tang, D.J. Nikolic-Paterson, H.Y. Lan, Macrophages: versatile players in renal inflammation and fibrosis, Nat. Rev. Nephrol. 15 (2019) 144–158, https://doi.org/10.1038/s41581-019-0110-2.
[4] L. Li, L. Huang, S.S. Sung, A.L. Vergis, D.L. Rosin, C.E. Rose, P.I. Lobo, M.D. Okusa, The chemokine receptors CCR2 and CX3CR1 mediate monocyte/macrophage trafficking in kidney ischemia-reperfusion injury, Kidney Int. 74 (2008) 1526–1537, https://doi.org/10.1038/ki.2008.500.
[5] T. Baudoux, C. Husson, E. De Prez, I. Jadot, M.H. Antoine, J.L. Nortier, J.M. Hougardy, CD4^{+} and CD8^{+} T cells exert regulatory properties during experimental acute aristolochic acid nephropathy, Sci. Rep. 8 (2018) 5334, https://doi.org/10.1038/s41598-018-23565-2.
[6] T. Kawakami, J. Lichtnekert, L.J. Thompson, P. Karna, H. Bouabe, T.M. Hohl, J.W. Heinecke, S.F. Ziegler, P.J. Nelson, J.S. Duffield, Resident renal mononuclear phagocytes comprise five discrete populations with distinct phenotypes and functions, J. Immunol. 191 (2013) 3358–3372, https://doi.org/10.4049/jimmunol.1300342.
[7] R.M. Steinman, Z.A. Cohn, Identification of a novel cell type in peripheral lymphoid organs of mice. I. Morphology, quantitation, tissue distribution, J. Exp. Med. 137 (1973) 1142–1162.
[8] K. Inaba, W.J. Swiggard, R.M. Steinman, N. Romani, G. Schuler, C. Brinster, Isolation of dendritic cells (Chapter 3), Curr. Protoc. Im. (2009) im0307s86, , https://doi.org/10.1002/0471142735 Unit 3.7.
[9] J.M. Austyn, D.F. Hankins, C.P. Larsen, P.J. Morris, A.S. Rao, J.A. Roake, Isolation and characterization of dendritic cells from mouse heart and kidney, J. Immunol. 152 (1994) 2401–2410.
[10] M. Clements, M. Gershenovich, C. Chaber, J. Campos-Rivera, P. Du, M. Zhang, S. Ledbetter, A. Zuk, Differential Ly6C expression after renal ischemia-reperfusion identifies unique macrophage populations, J. Am. Soc. Nephrol. 27 (2016) 159–170, https://doi.org/10.1681/ASN.2014111138.
[11] J. Menke, J.A. Lucas, G.C. Zeller, M.E. Keir, X.R. Huang, N. Tsuboi, T.N. Mayadas, H.Y. Lan, A.H. Sharpe, V.R. Kelley, Programmed death 1 ligand (PD-L) 1 and PD-L2 limit autoimmune kidney disease: distinct roles, J. Immunol. 179 (2007) 7466–7477.
[12] M.T. Gandolfo, H.R. Jang, S.M. Bagnasco, G.J. Ko, P. Agreda, S.R. Satpute, M.T. Crow, L.S. King, H. Rabb, Foxp3+ regulatory T cells participate in repair of ischemic acute kidney injury, Kidney Int. 76 (2009) 717–729, https://doi.org/10.1038/ki.2009.259.

[13] J.H. Baek, R. Zeng, J. Weinmann-Menke, M.T. Valerius, Y. Wada, A.K. Ajay, M. Colonna, V.R. Kelley, IL-34 mediates acute kidney injury and worsens subsequent chronic kidney disease, J. Clin. Invest. 125 (2015) 3198–3214, https://doi.org/10.1172/JCI81166.

[14] H.R. Jang, H. Rabb, Immune cells in experimental acute kidney injury, Nat. Rev. Nephrol. 11 (2015) 88–101, https://doi.org/10.1038/nrneph.2014.180.

[15] X. Peng, J. Zhang, Z. Xiao, Y. Dong, J. Du, CX3CL1-CX3CR1 interaction increases the population of Ly6C^{-}CX3CR1^{hi} macrophages contributing to unilateral ureteral obstruction-induced fibrosis, J. Immunol. 195 (2015) 2797–2805, https://doi.org/10.4049/jimmunol.1403209.

[16] J.D. Zhang, M.B. Patel, R. Griffiths, P.C. Dolber, P. Ruiz, M.A. Sparks, J. Stegbauer, H. Jin, J.A. Gomez, A.F. Buckley, W.S. Lefler, D. Chen, S.D. Crowley, Type 1 angiotensin receptors on macrophages ameliorate IL-1 receptor-mediated kidney fibrosis, J. Clin. Invest. 124 (2014) 2198–2203, https://doi.org/10.1172/JCI61368.

[17] M.C. Green, L.D. Shultz, Motheaten, an immunodeficient mutant of the mouse. I. Genetics and pathology, J. Hered. 66 (1975) 250–258.

[18] T. Kaneko, Y. Saito, T. Kotani, H. Okazawa, H. Iwamura, M. Sato-Hashimoto, Y. Kanazawa, S. Takahashi, K. Hiromura, S. Kusakari, Y. Kaneko, Y. Murata, H. Ohnishi, Y. Nojima, K. Takagishi, T. Matozaki, Dendritic cell-specific ablation of the protein tyrosine phosphatase Shp1 promotes Th1 cell differentiation and induces autoimmunity, J. Immunol. 188 (2012) 5397–5407, https://doi.org/10.4049/jimmunol.1103210.

[19] L.I. Pao, K.P. Lam, J.M. Henderson, J.L. Kutok, M. Alimzhanov, L. Nitschke, M.L. Thomas, B.G. Neel, K. Rajewsky, B cell-specific deletion of protein-tyrosine phosphatase Shp1 promotes B-1a cell development and causes systemic autoimmunity, Immunity 27 (2007) 35–48, https://doi.org/10.1016/j.immuni.2007.04.016.

[20] T. Tomizawa, Y. Kaneko, Y. Saito, H. Ohnishi, J. Okajo, C. Okuzawa, T. Ishikawa-Sekigami, Y. Murata, H. Okazawa, K. Okamoto, Y. Nojima, T. Matozaki, Resistance to experimental autoimmune encephalomyelitis and impaired T cell priming by dendritic cells in Src homology 2 domain-containing protein tyrosine phosphatase substrate-1 mutant mice, J. Immunol. 179 (2007) 869–877.

[21] W. Yumura, M. Itabashi, A. Ishida-Okawara, K. Tomizawa, J. Yamashita, Y. Kaneshiro, H. Nihei, K. Suzuki, A novel mouse model for MPO-ANCA-associated glomerulonephritis, Microbiol. Immunol. 50 (2006) 149–157.

[22] H.E. Chen, S. Chang, T. Trub, B.G. Neel, Regulation of colony-stimulating factor 1 receptor signaling by the SH2 domain-containing tyrosine phosphatase SHPTP1, Mol. Cell Biol. 16 (1996) 3685–3697.